

# An Ionization Chamber Shower Detector for the LHC Luminosity Monitor

J. F. Beche, M. T. Burks, P. S. Datte, M. Haguenaue, P. F. Manfredi, J. E. Millaud, M. Placidi,

L. Ratti, V. Re, V. J. Riot, H. Schmickler, V. Speziali and W. C. Turner

**Abstract--** The front IR quadrupole absorbers (TAS) and the IR neutral particle absorbers (TAN) in the high luminosity insertions of the Large Hadron Collider (LHC) each absorb approximately 1.8 TeV of forward collision products on average per pp interaction ( $\sim 235W$  at design luminosity  $10^{34} \text{cm}^{-2}\text{s}^{-1}$ ). This secondary particle flux can be exploited to provide a useful storage ring operations tool for optimization of luminosity. A novel segmented, multi-gap, pressurized gas ionization chamber is being developed for sampling the energy deposited near the maxima of the hadronic/ electromagnetic showers in these absorbers. The system design choices have been strongly influenced by optimization of signal to noise ratio and by the very high radiation environment. The ionization chambers are instrumented with low noise, fast, pulse shaping electronics to be capable of resolving individual bunch crossings at 40 MHz. Data on each bunch are to be separately accumulated over multiple bunch crossings until the desired statistical accuracy is obtained.

---

Manuscript received Nov. 6, 2000. Rev. Nov. 25, 2001. This work was supported by the Director, Office of Energy Research, Office of High Energy and Nuclear Physics, Division of High Energy Physics, of the U.S. Dept. of Energy under Contract No. DE-AC03-76SF00098.

J. F. Beche is with the Lawrence Berkeley National Laboratory, Berkeley, CA 94720 USA (telephone: 510-486-4164, e-mail: [JFBeche@lbl.gov](mailto:JFBeche@lbl.gov)).

M. T. Burks is with the Lawrence Berkeley National Laboratory, Berkeley, CA 94720 USA (telephone: 510-486-6219, e-mail: [MTBurks@lbl.gov](mailto:MTBurks@lbl.gov)).

P. S. Datte is with the Lawrence Berkeley National Laboratory, Berkeley, CA 94720 USA (telephone: 510-486-2906, e-mail: [PSDatte@lbl.gov](mailto:PSDatte@lbl.gov)).

M. Haguenaue is with Ecole Polytechnique, F-91128 Palaiseau Cedex 09 France, (telephone: 41 22 76 77198, e-mail: [Maurice.Haguenaue@cern.ch](mailto:Maurice.Haguenaue@cern.ch)).

P. F. Manfredi is with the Lawrence Berkeley National Laboratory, Berkeley, CA 94720 USA (telephone: 510-486-7786, e-mail: [PManfredi@lbl.gov](mailto:PManfredi@lbl.gov)).

J. E. Millaud is with the Lawrence Berkeley National Laboratory, Berkeley, CA 94720 USA (telephone: 510-486-4169, e-mail: [JEMillaud@lbl.gov](mailto:JEMillaud@lbl.gov)).

M. Placidi is with CERN, CH-1211, Geneva 23 Switzerland (telephone: 41 22 76 76638, e-mail: [Massimo.Placidi@cern.ch](mailto:Massimo.Placidi@cern.ch)).

L. Ratti is with the University of Pavia – INFN Pavia, Pavia, Italy (telephone: 39 0382 505.222, e-mail: [L.ratti@ele.unipv.it](mailto:L.ratti@ele.unipv.it)).

V. Re is with the University of Bergamo – INFN Bergamo, Bergamo, Italy (telephone: 39 035 277311, e-mail: [valere@unibg.it](mailto:valere@unibg.it)).

V. J. Riot is with the Lawrence Berkeley National Laboratory, Berkeley, CA 94720 USA (telephone: 510-486-2704, e-mail: [VJRiot@lbl.gov](mailto:VJRiot@lbl.gov)).

H. Schmickler is with CERN, CH-1211, Geneva 23 Switzerland (telephone number: 41 22 76 77078, e-mail: [Hermann.Schmickler@cern.ch](mailto:Hermann.Schmickler@cern.ch)).

V. Speziali is with the University of Pavia – INFN Pavia, Pavia, Italy (telephone: 39 0382 505.216, e-mail: [speziali@ele.unipv.it](mailto:speziali@ele.unipv.it)).

W. C. Turner is with the Lawrence Berkeley National Laboratory, Berkeley, CA 94720 USA (telephone: 510-486-7385, e-mail: [WCTurner@lbl.gov](mailto:WCTurner@lbl.gov)). Corresponding author.

At design luminosity approximately  $2 \times 10^{34}$  bunch crossings will suffice for a 1% luminosity measurement. In this paper we report the first experimental results of the ionization chamber and analog electronics. Single 450GeV protons from the SPS at CERN are used to simulate the hadronic/electromagnetic showers produced by the forward collision products from the interaction regions of the LHC.

## I. INTRODUCTION

THE feasibility of utilizing the very forward flux of secondary particles from IP interactions that are intercepted by the neutral particle and front quadrupole absorbers (TAN and TAS) of the LHC for the bunch-by-bunch measurement and optimization of luminosity has been discussed in previous reports.[1,2] The TAN and TAS absorbers have also been described previously.[3] It is proposed to instrument the neutral particle and front quadrupole absorbers with fast, low noise detectors that sample the energy deposited in the showers produced by the interaction products from the IP. A pressurized, segmented, multi-gap gas ionization chamber coupled with a radiation hard cable to a low noise, cold termination bipolar transistor preamplifier and pulse shaper have been chosen to meet the constraints imposed by radiation, bandwidth and signal to noise ratio.[4] The proposed system provides a fast relative luminosity monitor that can be periodically calibrated either by simultaneous measurement of the beam emittance and bunch intensity or against another absolute measurement of luminosity. The advantages of the proposed technique are that it is fast and that it is technologically relatively simple to implement. A 1% measurement of the luminosity of each of the 2835 colliding bunch pairs of the LHC can be carried out in  $\sim 2000$  turns. The instrumentation would be used as a storage ring operations tool to keep the LHC operating near optimum luminosity. In this report we describe the first experimental measurements of this system utilizing single 450GeV protons to simulate the hadronic/electromagnetic showers induced by the flux of particles from single pp interactions in the LHC. The following three sections of the report describe; (1) the experimental equipment, (2) the simulations of the hadronic/electromagnetic showers and of the electronics and (3) the experimental results. The report ends with a section on conclusions.

## II. DESCRIPTION OF EXPERIMENTAL EQUIPMENT

### A. Ionization chamber

A schematic of the ionization chamber is shown in Fig. 1. The ionization chamber is segmented into quadrants; each quadrant consists of sixty 0.5mm gaps separated by 1.0mm thick Cu plates. The 0.5mm gap width has been chosen so that the sum of the time for ionization electrons to drift across the gap and the amplifier shaping time is less than the 25nsec bunch spacing of the LHC. The active area of the plates is 48mm x 48mm and constrained by the requirement of fitting between the two beam tubes in the neutral particle absorbers of the high luminosity insertions of LHC. The stack of plates in each quadrant is connected electrically 10 in parallel, 6 in series to achieve a detector capacitance  $C_d \sim 50\text{pF}$ . The precise value of the detector capacitance is chosen by consideration of signal to noise ratio of the combined system capacitive detector + cable ( $R_0 = 50\text{Ohms}$ ,  $\sim 10\text{nsec}$  delay) + amplifier ( $\tau = 2.5\text{nsec}$  shaping time).[4] In order that the connecting cable does not degrade the signal to noise ratio of the system it is necessary to choose the ratio of shaping time to detector rise time so that  $\tau/R_0C_d \sim 1$ , thus leading to  $C_d \sim 50\text{pF}$ . The signal to noise ratio of the detector depends linearly on the gas pressure and is less sensitive to other parameters of the system. For this reason the ionization chamber is to be pressurized with up to 10 atmospheres of  $\text{Ar}+1\%\text{N}_2$ .

### B. Analog electronics

A schematic of the front-end preamplifier is shown in Fig. 2. The input stage has four transistors in parallel to reduce the rms noise of the input stage by a factor of two. The front-end preamplifier has a cold termination with broad band input impedance  $R_{in} = \frac{1}{g_m} \frac{C_1}{C_2} \approx 50\text{ Ohms}$ , where  $g_m = 0.2\text{A/V}$  is the transconductance of the four parallel transistors and the capacitors are labeled in Fig. 2.[5] The output of the front-end preamplifier feeds a differentiator-integrator pulse shaping network and output amplifier for driving a 50Ohm cable to the data acquisition system.

### C. Setup in a 450 GeV proton beam

Fig. 3 shows a schematic of the experimental setup in the SPS H4 beam area at CERN. A low intensity beam of 450GeV protons is incident on an array of scintillation counters and wire chambers that characterize the beam followed by a variable thickness absorber of 25cm x 25cm, 2.5cm thick Fe plates and the ionization chamber. The distance from the scintillation counters to the front of the absorber was 8.5m.

The ionization chamber detects the ionizing particles of the hadronic/electromagnetic showers exiting the absorber. The SPS operates with a 2.4sec slow extraction spill repeated every 14.4sec. The intensity of the beam was typically  $3-4 \times 10^5$  protons per spill. Data acquisition of the ionization chamber pulse was triggered by either a double coincidence between the 5mm x 5mm and 50mm x 50mm scintillation

counters or a triple coincidence of the ionization detector with these two counters. With the time base set at 500nsec per event, the data acquisition system was limited to acquiring 240 events per spill.

## III. SIMULATIONS

### A. Shower simulations

The average properties of hadronic/electromagnetic showers initiated by a 450GeV proton and propagating in an Fe absorber have been calculated with the MARS code.[6] Table I gives the average flux and mean energy of particles in the shower of a single 450GeV proton at a depth of 22cm in Fe. The energies in Table I include the rest masses of the particles. Relativistic electrons and positrons dominate the charged particle flux, accounting for  $130.2 + 85.9 = 216.1$  of the total 237 charged particles. The transverse spatial profile of electrons and positrons and their kinetic energy distribution are given in Figs. 4 and 5 respectively. The width of the spatial profile is solely due to the spreading of the shower since the incident proton beam has been simulated with zero width. The rms width of the shower in Fig. 4 is  $\sim 8.2\text{mm}$  with tails extending to  $\pm 4\text{cm}$ .

The maximum deposition of shower energy due to ionization is calculated to be  $0.55\text{GeV/gm}$  per incident 450GeV proton and to occur on the shower axis at a depth of  $z = 22\text{cm}$ . Integrated over the transverse plane at  $z = 22\text{cm}$ , the ionization energy loss per unit axial length is  $0.50\text{GeV-cm}^2/\text{gm}$ , with axial length expressed in units of  $\text{gm/cm}^2$ . Dividing by the minimum ionization energy loss in Fe,  $dE/dz_{\text{min}} = 1.45\text{MeV/gm-cm}^2$ , the equivalent flux of minimum ionizing particles (mips) is  $0.5 \times 10^3 / 1.45 = 345$ . On average then the 237 particles in Table I produce an ionization energy loss  $\langle dE/dz \rangle = 1.45 \times dE/dz_{\text{min}}$ .

The shower simulations may be used to estimate the expected average induced electron charge collected from the ionization chamber per proton shower. Since the chamber gaps are connected 10 in parallel, 6 in series the number of electron ion pairs produced in ten 0.5mm gaps is what we want to estimate. A minimum ionizing particle produces 97 electron ion pairs in Argon at one atmosphere pressure. At one atmosphere Argon pressure the average number of electron-ion pairs produced per proton shower in ten 0.5mm gaps is  $345 \times 97 \times 10 \times 0.05 = 1.67 \times 10^4$ . The average induced charge of electrons collected during a pulse is one half of this or  $8.3 \times 10^3$  e<sup>-</sup>/proton shower.

### B. Circuit simulations

A circuit simulation of the front-end electronics and pulse shaper is shown in Fig. 6. The simulation used a detector capacitance 50pF connected to the preamplifier by a coaxial cable with physical characteristics close to the actual rad-hard cable employed in the experiment. Fig. 6(a) is the triangular input pulse of ionization electrons with base width 25nsec and total charge  $2.6 \times 10^4$ e. Referring to the previous Sec. III A this charge corresponds to the shower maximum at 3.1 atmospheres pressure in the ionization chamber. Fig. 6(b)

shows the output of the preamplifier reaching a peak value of 2.9mV at 22.0nsec after the passage of the shower.

Fig. 6(c) shows the output of the pulse shaper and cable driver reaching a peak amplitude 41mV in 14.5nsec and having a base width  $\sim 37.0$ nsec. For the application in LHC further optimization is needed to reduce the base width to less than 25nsec. The transfer function of the system is calculated from the amplitude of the output pulse in Fig. 6;  $0.041\text{V}/2.6 \times 10^4 = 1.6 \times 10^{-6}\text{V/e}$ .

#### IV. EXPERIMENTAL RESULTS

##### A. Electron drift velocity measurements

A drift chamber with a photo-cathode illuminated by a 337nm pulsed laser has been used to measure the drift velocity of electrons for argon nitrogen mixtures as a function of the ratio of electric field strength to gas pressure.[7] The results are shown in Fig. 7. The electron drift velocity of the Ar+1%N<sub>2</sub> mixture reaches a saturated value 2.3cm/ $\mu\text{sec}$  at  $E/p = 850\text{V/cm}$ . Increasing the N<sub>2</sub> fraction increases the saturation drift velocity and the  $E/p$  ratio at saturation. All of the beam data reported in this paper were taken with the Ar+1%N<sub>2</sub> mixture and the electric field strength 6000V/cm provided by 300V batteries. The absolute pressure was varied from 3 to 11 atmospheres corresponding to  $E/p$  varying from 545 to 2000V/cm. For the future it is worthwhile to consider increasing the N<sub>2</sub> fraction to decrease the electron collection time and relax the requirement on the shaping time of the differentiator-integrator.

##### B. Electronics bench tests

Bench top measurements of the transfer function, rms noise voltage and equivalent noise charge (ENC) of the as built analog electronics used in the beam tests at CERN were carried out. With 2.5nsec shaping time the transfer function of the as built circuit for a triangular shaped input pulse with base width 25nsec (Fig. 6a) was measured to be  $1.1 \times 10^{-6}\text{V/e}$ . The rms noise voltage for a "delta" function input pulse was measured to be 2.25mV and the corresponding rms equivalent noise charge was measured to be  $\sim 2,300\text{e}$ . For a 25nsec wide triangular pulse and 2.5nsec shaping time the ballistic deficit was measured to be 2.71. The equivalent noise charge for this triangular waveform corrected for the ballistic deficit is then  $2.71 \times 2,300 = 6,233\text{e}$ . On the basis of these measurements and the MARS simulations at 3.1 atmospheres Ar + 1%N<sub>2</sub> and with the ionization chamber placed at the shower maximum one expects a mean pulse height  $1.1 \times 10^{-6}\text{V/e} \times 2.6 \times 10^4\text{e} = 0.028\text{V}$  and signal to noise ratio  $2.6 \times 10^4/6,233 = 4.2$ .

##### C. Pulse shapes and spectra

###### 1) Typical pulses

Typical measured waveforms for showers induced by single protons are shown in Fig. 8. The waveforms were taken with a single quadrant of the ionization chamber connected and the quadrant centered on the proton beam line. Capacitive coupling of noise between quadrants prevented

operating them simultaneously. For these data the absorber had 11 Fe plates (28cm) and the absolute gas pressure was 900kPa of Ar + 1%N<sub>2</sub>. Fig. 8(a) is an average over 9600 single proton showers, Fig. 8(b) is a waveform of a single shower and Fig. 8(c) is a noise waveform with no ionization in the chamber. Comparing Fig. 8(a) to Figs. 8(b) and 8(c) the effect of averaging the noise is clearly evident. For these events the data acquisition system was triggered by a two fold coincidence between the 5mm x 5mm and 50mm x 50mm scintillation counters so there is no threshold condition on the ionization chamber pulses. The peak amplitude of the average waveform is 0.012V and the base width is  $\sim 175$ nsec. One notices immediately that the pulse height of the average proton shower is less and the pulse width is greater than expected. In addition one notes that there are secondary peaks on the falling waveform occurring 28.6, 67.7, 94.9 and 138nsec after the first peak. Nevertheless it is clear that signals from showers induced by single protons are discernable even without averaging. The rms noise voltage in Fig. 8(c) is 4.8mV; the ratio of the mean pulse height to the rms noise level is  $12.4/4.8 = 2.6$ .

###### 2) Pulse height spectra

Pulse height spectra are given in Fig. 9(a) for the 9,600 single proton shower events contributing to the average waveform in Fig. 8(a) and in Fig. 9(b) for 1,920 noise events with no ionization in the chamber. The profiles have bin width 0.07937mV and are normalized so the sum over bins equals 1.0. The mean pulse height of the shower spectrum is 16.2mV and of the noise spectrum 11.0mV. The non-Gaussian Landau tail of the ionization spectrum is clearly evident in Fig. 9(a).

###### 3) Supporting details – beam size, timing plateau, horizontal and vertical scans through the beam

The transverse beam profiles of the 450GeV proton beam are measured with charge integrating wire chambers with wire spacing 2mm.[8] The results of typical vertical and horizontal profiles are shown in Figs. 10(a) and 10(b) respectively. These profiles were reasonably stable during the seven days of operation since no changes were made to the beam optics. The rms widths of the beam profiles are 11mm and 7.9mm respectively in the vertical and horizontal directions.

An array of scalers was used to monitor the counting rates of the ionization chamber, the upstream scintillation counters and various coincidences between them. The timing of the scintillation counters relative to one another had been previously established and it only remained to establish the timing of the ionization chamber. A timing plateau of the ionization chamber in coincidence with the 5mm x 5mm and 50mm x 50mm scintillation counters is shown in Fig. 11. The vertical axis is the rate of triple coincidences between the ionization chamber and scintillation counters divided by the rate of double coincidences of the scintillation counters, plotted as a function of timing of the ionization chamber relative to the coincidence gate. The timing of the ionization pulse is normally set at  $t = 0$  in Fig. 11.

With the timing of the ionization chamber fixed relative to the scintillation counters as just described, the response of the ionization chamber moving vertically and horizontally through the proton beam was measured. The scintillation counters remain fixed in position on the proton beamline as the ionization chamber is moved. The results are plotted in Figs. 12(a) and 12(b). Again the counting ratio of triple coincidences of ionization detector with scintillation counters to the double coincidences of the scintillation counters is plotted, this time versus the position of the table on which the ionization chamber and absorber are supported. The profiles in Fig. 12 have FWHMs  $\sim 48\text{mm}$ , consistent with the  $48\text{mm} \times 48\text{mm}$  active area of the ionization chamber.

#### D. Pulse height versus gas pressure

Data were recorded varying the absolute pressure of Ar + 1%N<sub>2</sub> from 300kPa to 1100kPa while triggering the data acquisition system by a triple coincidence between the ionization chamber and scintillation counters. Under these circumstances the ionization chamber threshold for recording an event was 26.16mV. The data are then analyzed by selecting recorded events with a threshold varying linearly with pressure corresponding to 26.16, 43.6, 61.0, 78.4 and 95.9mV for pressures 300, 500, 700, 900 and 1100kPa respectively. The mean waveforms of these events are shown in Fig. 13(a) and the peak heights are plotted in Fig. 13(b). The peak heights are fitted with a straight line  $h = a + bP$  with slope  $b = 9.03 \pm 0.30 \times 10^{-5} \text{V/kPa}$  and intercept consistent with zero  $a = 2.6 \pm 2.2 \times 10^{-3} \text{kPa}$ .

#### E. Ionization chamber counting rate versus absorber thickness

The counting rate of the ionization chamber per proton spill normalized to the counting rate of the  $50\text{mm} \times 50\text{mm}$  scintillation counter is plotted in Fig. 14 as a function of the thickness of Fe plates in the absorber. The data show a shower maximum corresponding to a Fe plate thickness  $\sim 15\text{cm}$ . Most of our data was taken with a  $28\text{cm}$  thickness of Fe plates, partially accounting for the less than expected signal amplitude. Extrapolating the data in Fig. 14 to zero ionization chamber counting rate, one concludes that the combined effect of the other material in the beam – Al box holding the plates, SS vacuum flange and Cu plates of the ionization chamber – is equivalent to an additional thickness of  $5\text{cm}$  of Fe, bringing the effective thickness of Fe at the shower maximum to  $\sim 20\text{cm}$ .

## V. CONCLUSIONS

In this paper we have given a status report on our work to develop a 40MHz ionization chamber detector for use as storage ring operations tool for measuring and optimizing the bunch-by-bunch luminosity of the LHC. The first prototype has been built and tested in a 450GeV proton beam that simulates the hadronic/electromagnetic showers anticipated in the LHC application of these detectors. In the SPS H4 beam tests the following observations were made:

- feasibility of the ionization chamber to detect hadronic/electromagnetic showers initiated by a single 450GeV proton was demonstrated,
- linear scaling of signal amplitude with ionization chamber pressure was verified from 300–1100kPa Ar+1%N<sub>2</sub>,
- position of the shower maximum was measured to occur with an effective thickness of 20cm of Fe in front of the ionization chamber.

Shower simulations have shown that the flux of ionizing particles produced by the showers of single 450GeV protons are nearly equal to that anticipated from a single pp interaction in the LHC. It therefore follows that the ionization chamber that is being developed will be sensitive to single pp interactions in the LHC and capable of operating over the full range of luminosity that is anticipated for LHC ( $10^{28} - 2.5 \times 10^{34} \text{cm}^{-2} \text{sec}^{-1}$ ).

Several issues have been identified which need further study and development work including:

- reducing or eliminating capacitive coupling of noise between quadrants to allow simultaneous operation of all the quadrants and
- reducing the baseline pulse width from its present value of 175nsec to  $< 25\text{nsec}$  required for 40 MHz operation.

Capacitive coupling can be eliminated rather simply by inserting ground planes between the quadrants. In the rush of preparations to meet the scheduled beam running time we were not able to do a thorough job of measuring the effective impedance of the ionization chamber and the input impedance of the front-end preamplifier. Since the beam tests were performed we have embarked on these measurements and found discrepancies with expected values. Preliminary simulations and bench top measurements suggest these are responsible for the wider than desired output pulse and also for the secondary peaks observed in Fig. 8(a). We intend to pursue this study, modify the system and test it again in the setup that has been described in this paper.

## VI. ACKNOWLEDGMENT

We would like to thank Thomas Ruf, coordinator for SPS extracted beams and Per Grafstrom, liaison physicist for SPS H4 beam operations, for support and help in carrying out the experiments described in this report.

## VII. REFERENCES

- [1] W.C. Turner, "Instrumentation for the Absorbers in the Low Beta Insertions of LHC", LBNL-42180, (13 Aug. 1998).
- [2] W.C. Turner, P.S. Datte, P.F. Manfredi, J.E. Millaud, N.V. Mokhov, M. Placidi, V. Re and H. Schmickler, "Status Report on the Development of Instrumentation for Bunch by Bunch Measurement and Optimization of Luminosity in the LHC", Proc. of US LHC Collaboration Meeting on Accelerator Physics Experiments for Future Hadron Colliders, Brookhaven, 22-23 Feb. 2000.
- [3] W.C. Turner, E.H. Hoyer and N.V. Mokhov, "Absorbers for the High Luminosity Insertions of the LHC," Proc. Of EPAC 98", Stockholm, 1998, pg. 368.
- [4] W.C. Turner, M.T. Burks, P.S. Datte, P.F. Manfredi, J.E. Millaud, N.V. Mokhov, M. Placidi, L. Ratti, V. Re, H. Schmickler and V. Speziali, "Development of a detector for bunch by bunch measurement and optimization of luminosity in the LHC", Proc. of 8th Pisa Meeting on Advanced Detectors, Isola d'Elba, 21-27 May 2000.
- [5] E. Gatti and P.F. Manfredi, "Signal Coupling from a Semiconductor Detector to a Cold Termination Resistance Preamplifier Through a Cable or a Delay Line Transformer", IEEE Trans. Nucl. Sci., Vol. NS-25, 66-74. (1978)
- [6] N.V. Mokhov, "MARS Code Developments, Benchmarking and Applications," Proc. ICRS-9 Intl. Conf. on Radiation Shielding", Tsukuba, Japan, Oct. 1999, and references therein.
- [7] M. Burks, S. Trentalange, S. Margetis and H. Wieman, "Electron Drift Parameters in Dimethyl Ether", NIM A385, 519-522. (1997)
- [8] P. Dreesen and G. Vismara, "Integrating Wire Chambers for Beam Tuning in the CERN SPS Experimental Areas", CERN-SPS/EA/78-4. (1978)

Table I  
The flux and mean energy of shower particles per 450GeV  
proton at depth of 22cm in Fe.

particle	Flux per proton	Mean energy, MeV
$e^-$	130.2	75.2
$e^+$	85.9	109.8
$\pi^-$	6.9	6,500
$\pi^+$	8.0	7,820
$K^-$	0.74	7,988
$K^+$	0.78	10,812
p	4.4	39,031
n	23.2	2,121
$\gamma$	2743.5	14.0
All chg.	237.0	-

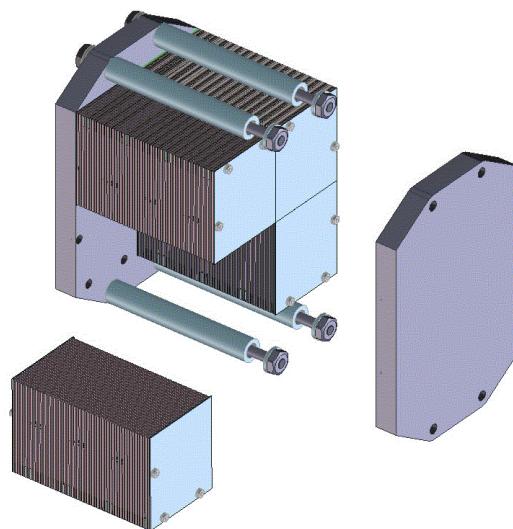


Fig 1: Schematic of the ionization chamber.

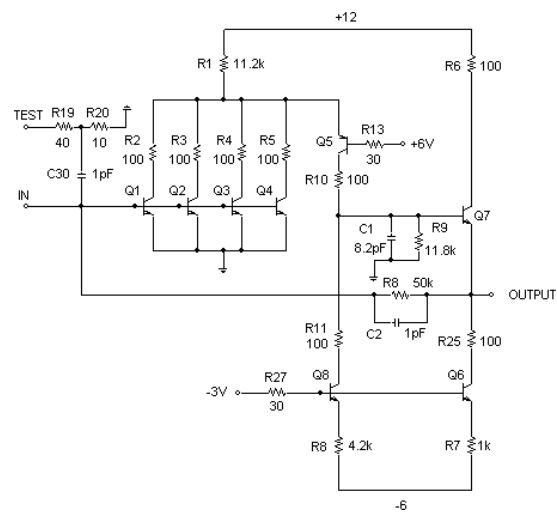


Fig. 2: Schematic of the front-end amplifier.

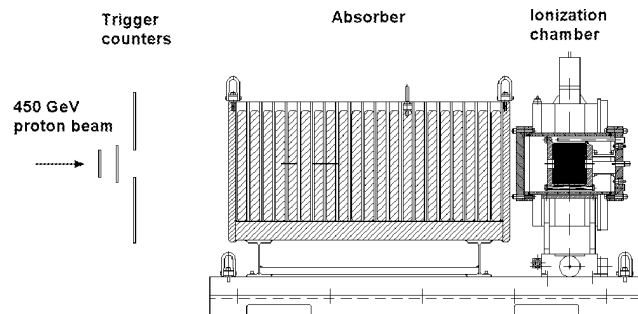


Fig. 3: Schematic of trigger counters, absorber and ionization chamber.

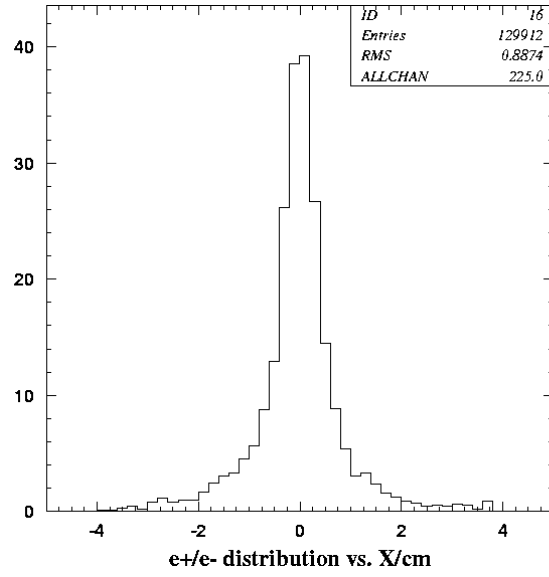


Fig. 4: The spatial profile of shower electrons and positrons at a depth of 22cm in Fe.

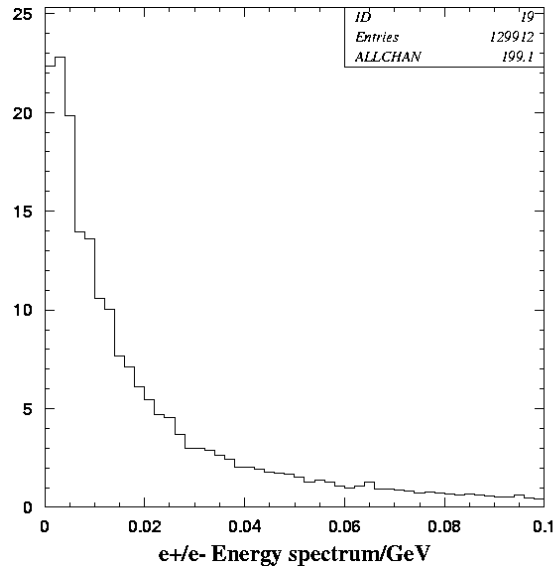


Fig. 5: The kinetic energy spectrum of shower electrons and positrons at a depth of 22cm in Fe.



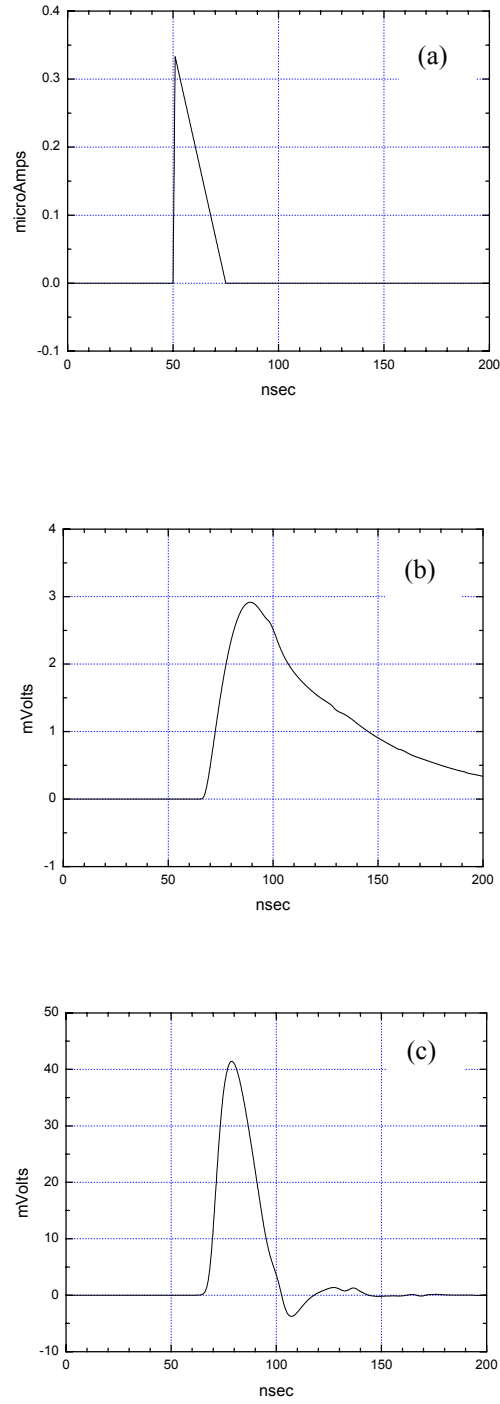


Fig. 6: Simulated output pulses of the front-end preamplifier and pulse shaper; (a) input current pulse of ionization electrons, (b) output pulse of front-end preamplifier and (c) output of pulse shaper and cable driver.

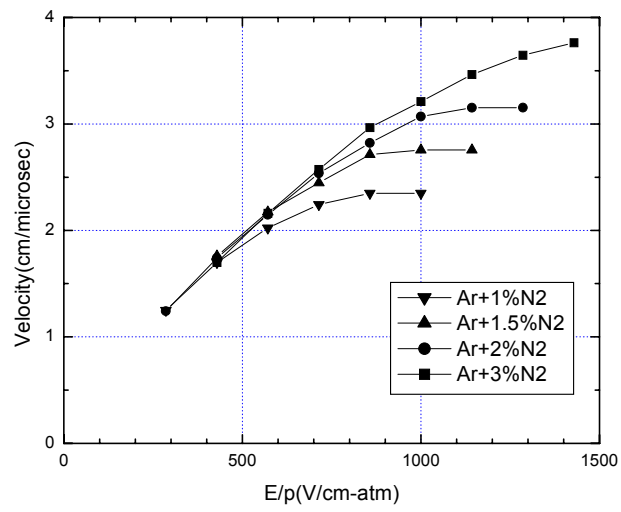


Fig. 7: Electron drift velocity versus  $E/p$  for mixtures of Ar and N<sub>2</sub>.

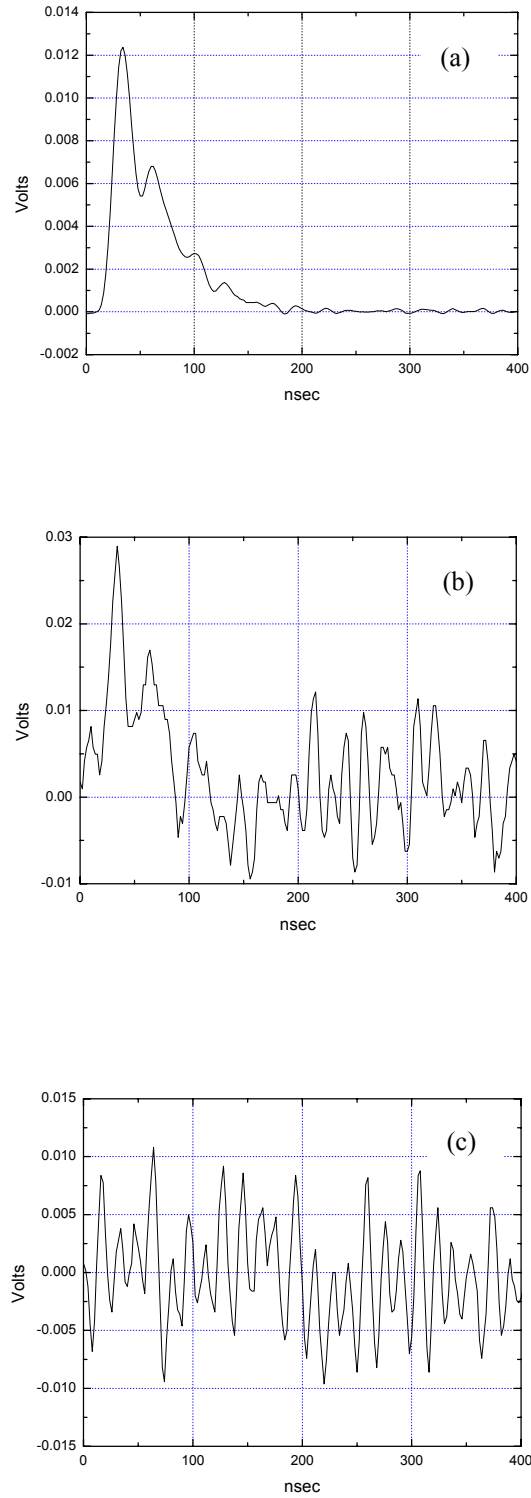


Fig. 8: Typical ionization chamber pulses: (a) averaged over 9600 single proton showers, pulse height = 12.4mV, 11 Fe plates, 900kPa abs. Ar+1%N<sub>2</sub>, (b) for a single proton shower, (c) for a single noise event with no ionizing particles in the chamber.

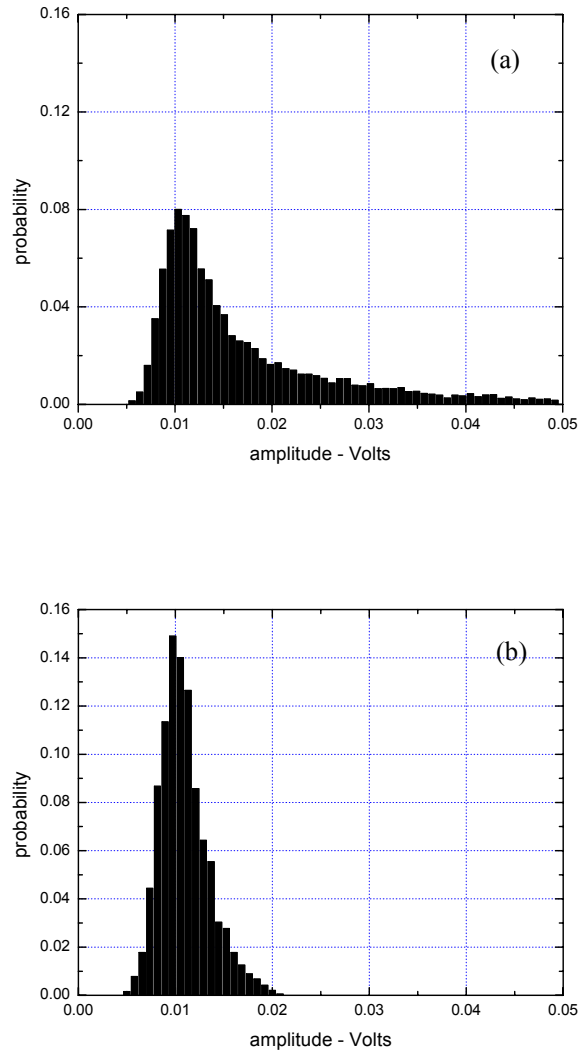


Fig. 9: Ionization chamber pulse height spectra, bin width = 0.7937mV; (a) 9600 single proton showers with 11 Fe plates, 900kPa abs Ar+1%N<sub>2</sub>, (b) 1,920 noise events.

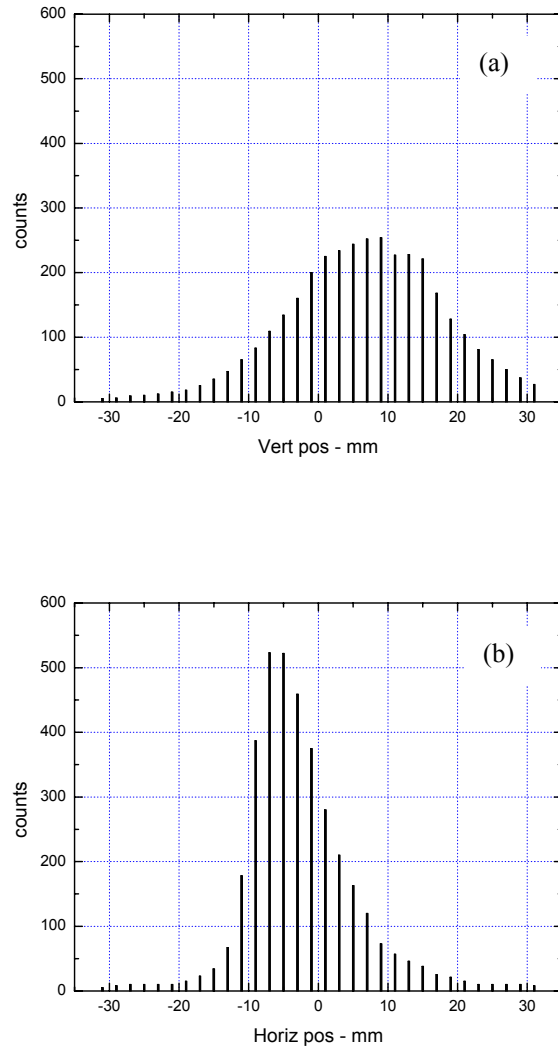


Fig. 10: (a) Vertical and (b) horizontal profiles of the 450 GeV proton beam.

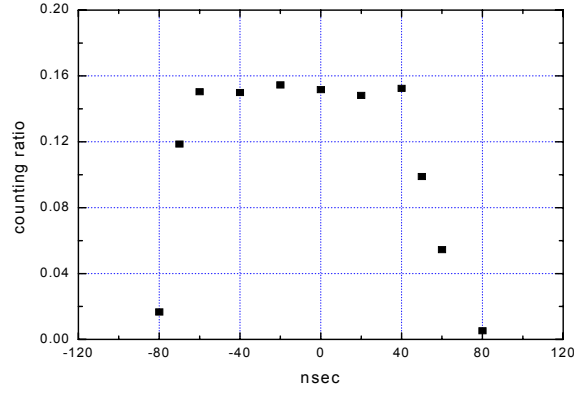


Fig. 11: A timing plateau of the ionization chamber in coincidence with the 5mm x 5mm and 50mm x 50mm scintillation counters.

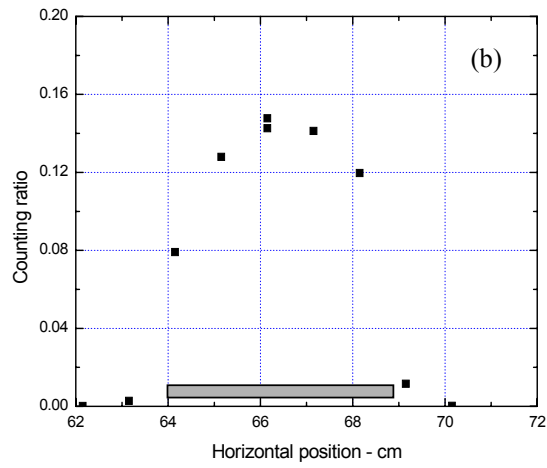
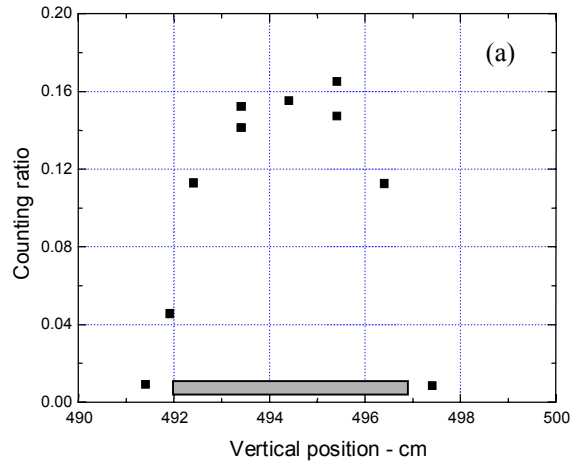


Fig. 12: (a) Vertical and (b) horizontal scans of the normalized ionization chamber counting rate as functions of the chamber position. The surveyed proton beamline is at  $H = 66.15\text{cm}$ ,  $V = 494.5\text{cm}$ .

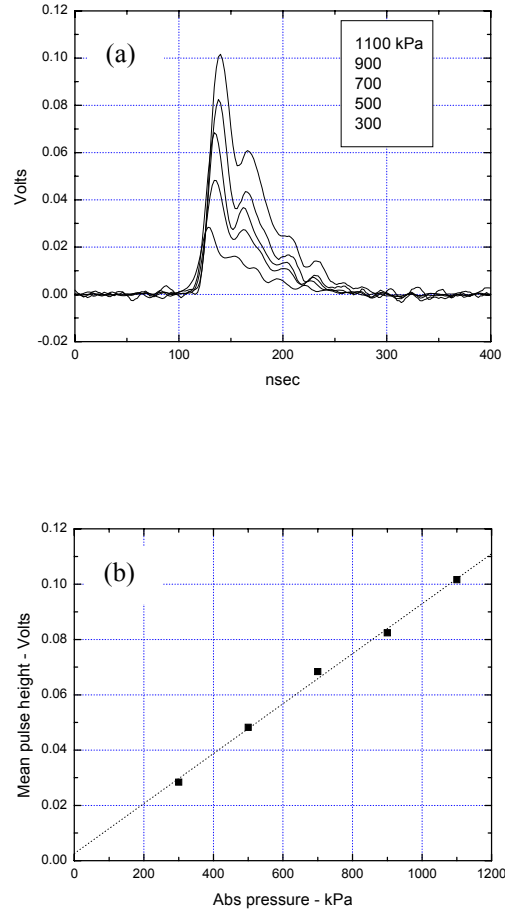


Fig. 13: (a) Mean Ionization chamber waveform for single 450GeV proton showers for gas pressures 300, 500, 700, 900 and 1100kPa Ar+1%N<sub>2</sub>, (b) pulse height of the mean ionization chamber waveform versus gas pressure.

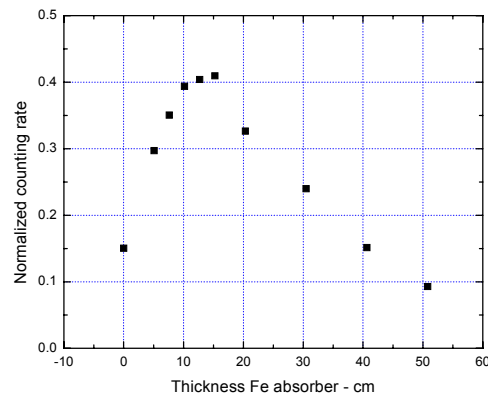


Fig. 14: Counting rate of the ionization chamber normalized to the 50mm x 50mm scintillation counter rate as function of Fe absorber thickness.